

The effect of shapes in input-state linearization for stabilization of nonprehensile planar rolling dynamic manipulation

Vincenzo Lippiello, Fabio Ruggiero, and Bruno Siciliano

Abstract—A control framework for nonprehensile planar rolling dynamic manipulation is derived in this paper. By rotating around the center of mass, the manipulator moves a part without grasping it but exploiting its dynamics. Given some assumptions on the shapes of both the object and the manipulator, a state transformation is found rendering the state-space system in a chain of integrators form without internal dynamics, allowing the possibility to exploit linear controls to stabilize the whole system. An analysis of the differential flatness property of the system is also provided. Simulations and experiments validate the derived framework.

I. INTRODUCTION

The robotic manipulation problem aims at finding a set of suitable controls to change the configuration of an object from an initial to a desired value. Such manipulation task can be achieved in a *nonprehensile*—the object is not grasped—and *dynamic*—dynamics is exploited to control the motion—way. This class of manipulation problems is still rather far from being fully solved and applied in robotic applications, while indeed there are several benefits [1]. As examples, vibratory platforms are employed in those industrial applications where it is not directly possible to manipulate the object by grasping, while dynamic nonprehensile manipulation tasks are also performed during surgery to push away arteries and reshape organs. Therefore, in order to perform similar tasks, the control design has to carefully take into account both the object and the robot dynamics. A typical approach to tackle a nonprehensile dynamic manipulation task is to divide complex actions into simpler subtasks, called *primitives*, such as rolling, throwing, catching, pushing, batting, and so on. This paper is focused on the nonprehensile planar rolling primitive, where an actuated manipulator of a given shape, referred to as *hand*, manipulates an object without grasping it through rotations. The object can only roll upon the hand's shape.

Nonprehensile manipulation tasks have been firstly introduced in robotics in [1], [2], [3]. Regarding the nonprehensile rolling primitive, the ball and plate and the ball and beam are the most investigated benchmark systems. The former consists of a ball rolling without slipping on an actuated plane. In such nonholonomic system, the controller steers

The research leading to these results has been supported by the RoDyMan project, which has received funding from the European Research Council FP7 Ideas under Advanced Grant agreement number 320992. The authors are solely responsible for the content of this manuscript.

V. Lippiello, F. Ruggiero, and B. Siciliano are with CREATE Consortium and with Department of Electrical Engineering and Information Technology, University of Naples Federico II, via Claudio 21, 80125, Naples, Italy. Authors are listed in alphabetical order. Corresponding author: Fabio Ruggiero, fabio.ruggiero@unina.it.

the ball by moving the plate from its initial configuration to a desired position along an admissible path [4]. A PID-based controller is employed in [5], while a sliding mode controller in [6]. The latter, instead, aims at stabilizing the position of a ball along the beam. No full state feedback linearization can be designed, but an approximated partial feedback linearization is proposed in [7]. An output feedback controller is introduced in [8]. A flatness based approach with an exact feedforward linearization (EFL) is introduced in [9]. The *butterfly* juggling task has been investigated in [10], [11], [12]. The stabilization of a disk free to roll on an actuated disk is introduced in [13], while an input-state linearization is proposed in [14]. Planning and control of rolling on general curved shapes is studied in [15]. Finally, nonprehensile rolling systems where the object's center of mass does not coincide with its geometric center are investigated in [16].

The scope of this manuscript is to find and apply a general diffeomorphism to achieve an input-state linearization of the whole dynamics. Such state transformation renders the system in the so-called *normal form* (i.e., a chain of integrators) without internal dynamics. Given some assumptions on the shapes of both the object and the hand, EFL is employed to stabilize the system. A connection with differential flatness theory is also considered. Case studies validate the approach through simulations and experiments, showing that the whole system has good performance even when the assumptions regarding the shapes are not satisfied.

Upon derivation of the general dynamic model for nonprehensile planar rolling manipulation, two main novelties are highlighted in the paper: (i) a link between nonprehensile planar rolling manipulation and differential flatness is established; (ii) given some assumptions on both the hand and object shapes, a diffeomorphism to build a unified theoretical framework to plan and control these tasks is derived.

II. MATHEMATICAL BACKGROUND

In order to make the paper self-contained, this section aims to recap some basic definitions (see [17] for further details). Consider a dynamic system in the affine state-space form

$$\dot{\mathbf{x}} = \mathbf{f}(\mathbf{x}) + \mathbf{b}(\mathbf{x})u, \quad (1)$$

with $\mathbf{x} \in \mathbb{R}^n$ and $u \in \mathbb{R}$ representing the state and the input, respectively, while $\mathbf{f} : \mathbb{R}^n \rightarrow \mathbb{R}^n$ and $\mathbf{b} : \mathbb{R}^n \rightarrow \mathbb{R}^n$ are two smooth vector fields. A system (1) is input-state linearizable if there exists a diffeomorphism $\phi : \Omega \rightarrow \mathbb{R}^n$, where $\Omega \subseteq \mathbb{R}^n$, and a feedback control law $u = \alpha(\mathbf{x}) + \beta(\mathbf{x})v$, such that the new state $\mathbf{z} = [z_1 \ z_2 \ \dots \ z_n]^\top = \phi(\mathbf{x})$ and input v

render the system (1) in the following normal form

$$\begin{cases} \dot{z}_i = z_{i+1} \\ \dot{z}_n = v, \end{cases} \quad (2a)$$

$$(2b)$$

with $i = 1, \dots, n-1$. The following theorem gives the conditions to verify whether (1) can be transformed in the normal form (2).

Theorem 1: The nonlinear system (1) is input-state linearizable if and only if there exists a region Ω where the following conditions hold:

- The controllability matrix $\mathbf{T} = [\mathbf{b}, \text{ad}_{\mathbf{f}}\mathbf{b}, \dots, \text{ad}_{\mathbf{f}}^{n-1}\mathbf{b}]$ is made by linearly independent vector fields in Ω .
- The set $[\mathbf{b}, \text{ad}_{\mathbf{f}}\mathbf{b}, \dots, \text{ad}_{\mathbf{f}}^{n-2}\mathbf{b}]$ is involutive in Ω .

Proof: See [17], Theorem 6.2. \blacksquare

Notice that $\text{ad}_{\mathbf{f}}^i \mathbf{b} = [\mathbf{f}, \text{ad}_{\mathbf{f}}^{i-1} \mathbf{b}]$, where $i = 1, 2, \dots$, $\text{ad}_{\mathbf{f}}^0 \mathbf{b} = \mathbf{b}$, and $[\cdot, \cdot]$ denotes the Lie bracket [17]. Theorem 1 is not constructive to find the diffeomorphism $\phi(\mathbf{x})$. Then, the following steps can be followed:

- In order to find z_1 in the diffeomorphism $\phi(\mathbf{x})$, the following equations have to hold

$$\frac{\partial z_1}{\partial \mathbf{x}} \text{ad}_{\mathbf{f}}^i \mathbf{b} = 0, \quad (3a)$$

$$\frac{\partial z_1}{\partial \mathbf{x}} \text{ad}_{\mathbf{f}}^{n-1} \mathbf{b} \neq 0, \quad (3b)$$

with $i = 0, \dots, n-2$.

- The complete transformation is given by

$$\mathbf{z} = \phi(\mathbf{x}) = \begin{bmatrix} z_1 & L_{\mathbf{f}} z_1 & \dots & L_{\mathbf{f}}^{n-1} z_1 \end{bmatrix}^T. \quad (4)$$

Notice that $L_{\mathbf{f}}^i h = L_{\mathbf{f}}(L_{\mathbf{f}}^{i-1} h)$, where $i = 1, 2, \dots$, $L_{\mathbf{f}}^0 h = h$ and $L_{\mathbf{f}} h$ denotes the Lie derivative. Finally, the transformation $u = \alpha(\mathbf{x}) + \beta(\mathbf{x})v$ renders (1) as in (2), where

$$\alpha(\mathbf{x}) = -\frac{L_{\mathbf{f}}^n z_1}{L_{\mathbf{b}} L_{\mathbf{f}}^{n-1} z_1}, \quad \beta(\mathbf{x}) = \frac{1}{L_{\mathbf{b}} L_{\mathbf{f}}^{n-1} z_1}. \quad (5)$$

III. MODELLING OF NONPREHENSILE PLANAR ROLLING

Extending what presented in [14], the modelling of a nonprehensile planar rolling manipulation system is now derived.

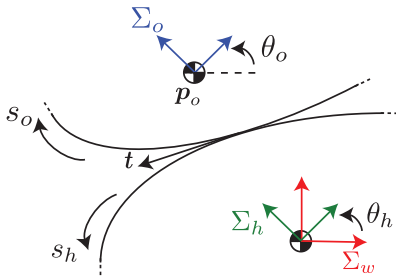


Fig. 1. A general nonprehensile planar rolling manipulation system. In red the world fixed frame Σ_w . In green the hand frame Σ_h , while in blue the object frame Σ_o , placed at the respective centres of mass.

Referring to Fig. 1, let Σ_w be the inertia world fixed frame, while let Σ_h be the frame attached to the hand, and Σ_o

the frame attached to the object: both are located at their respective centres of mass. Let $\theta_h \in \mathbb{R}$ be the angle of the hand in Σ_w , while $\mathbf{p}_o \in \mathbb{R}^2$ and $\theta_o \in \mathbb{R}$ are the position and the orientation, respectively, of Σ_o in Σ_w .

The shapes of both the object and the hand are represented through an arclength parametrization: $s_h \in \mathbb{R}$ and $s_o \in \mathbb{R}$ are the arclength parameters for the hand and the object, respectively. At least locally, the shapes should be of class \mathcal{C}^2 . Locally, any point of the hand's shape is given by $\mathbf{c}_h^h(s_h) = [u_h(s_h) \quad v_h(s_h)]^T \in \mathbb{R}^2$, expressed with respect to Σ_h , while any point of the object's shape is given by $\mathbf{c}_o^o(s_o) = [u_o(s_o) \quad v_o(s_o)]^T \in \mathbb{R}^2$, expressed with respect to Σ_o . Notice that s_h increases counterclockwise along the hand, while s_o increases clockwise along the object. With this choice, the pure rolling assumption is $\dot{s}_h = \dot{s}_o$. Without loss of generality, the frames Σ_w and Σ_h coincide at $\theta_h = 0$, the point $s_h = 0$ is at the intersection between the vertical (gravitational) axis of Σ_w and the hand's shape, *i.e.* $\mathbf{c}_h(0) = [0 \quad v_h(0)]^T$ in Σ_w , and thus $s_h = s_o$ at all times during rolling. Therefore, the contact location will be specified only by s_h throughout the remainder of the paper.

Assumption 1: The hand and the object maintain pure rolling contact for all the times.

The arclength parametrization implies the property $\|\mathbf{c}_h^{h'}\| = 1$, with the symbol $'$ indicating the derivative with respect to the parameter s_h . The same holds for $\mathbf{c}_o^o(s_h)$. At the contact point $\mathbf{c}_h^h(s_h)$, the tangent vector to the shapes is expressed as $\mathbf{t}^h(s_h) = \mathbf{c}_h^{h'} \in \mathbb{R}^2$ forming an angle $\phi_h(s_h) = \text{atan2}(v_h'(s_h), u_h'(s_h))$ in Σ_h . The same tangent can be expressed with respect to Σ_o with an angle $\phi_o(s_h) = \text{atan2}(v_o'(s_h), u_o'(s_h))$. The signed curvatures of the shapes are defined as

$$\kappa_h(s_h) = \phi_h'(s_h) = u_h'(s_h)v_h''(s_h) - u_h''(s_h)v_h'(s_h), \quad (6a)$$

$$\kappa_o(s_h) = \phi_o'(s_h) = u_o'(s_h)v_o''(s_h) - u_o''(s_h)v_o'(s_h). \quad (6b)$$

The relative curvature at the contact point is given by $\kappa_r(s_h) = \kappa_h(s_h) - \kappa_o(s_h)$. Notice that $\kappa_h(s_h) > 0$ and $\kappa_o(s_h) < 0$ denote convexity at the contact point for the hand and the object, respectively. Hence, $\kappa_r(s_h) > 0$ guarantees a single contact point at least locally [14]. The following constraint expresses the angle of the tangent $\mathbf{t}^h(s_h)$ with respect to Σ_w : $\theta_h + \phi_h(s_h) = \theta_o + \phi_o(s_h)$. Therefore, taking into account (6), the following relations hold

$$\theta_o = \theta_h + \phi_h(s_h) - \phi_o(s_h), \quad (7a)$$

$$\dot{\theta}_o = \dot{\theta}_h + \kappa_r(s_h)\dot{s}_h. \quad (7b)$$

The following constraint expresses instead the coincidence between the contact points on both the hand and the object

$$\mathbf{p}_h + \mathbf{R}(\theta_h)\mathbf{c}_h^h(s_h) = \mathbf{p}_o + \mathbf{R}(\theta_o)\mathbf{c}_o^o(s_h), \quad (8)$$

where $\mathbf{p}_h \in \mathbb{R}^2$ is the position of Σ_h in Σ_w , while $\mathbf{R}(\theta) \in SO(2)$ is the rotation matrix in the 2D space. Notice that the relation $\dot{\mathbf{R}}(\theta) = \mathbf{R}(\bar{\theta})\dot{\bar{\theta}}$ holds with $\bar{\theta} = \theta + \frac{\pi}{2}$.

Assumption 2: The hand can only rotate around its center of mass.

Therefore, without loss of generality, placing Σ_w at the hand's center of mass and taking into account (8) yield $\mathbf{p}_o = \mathbf{R}(\theta_h)\mathbf{c}_h^h(s_h) - \mathbf{R}(\theta_o)\mathbf{c}_o^o(s_h)$, and $\dot{\mathbf{p}}_o = \boldsymbol{\gamma}(\mathbf{q})\dot{\theta}_h + \boldsymbol{\eta}(\mathbf{q})\dot{s}_h = [\boldsymbol{\gamma}(\mathbf{q}) \quad \boldsymbol{\eta}(\mathbf{q})] \dot{\mathbf{q}}$, with $\mathbf{q} = [q_1 \quad q_2]^T = [\theta_h \quad s_h]^T$, and

$$\boldsymbol{\gamma} = \mathbf{R}(\bar{\theta}_h)\mathbf{c}_h^h - \mathbf{R}(\bar{\theta}_o)\mathbf{c}_o^o, \quad (9a)$$

$$\boldsymbol{\eta} = \mathbf{R}(\theta_h)\mathbf{c}_h^{h'} - \mathbf{R}(\theta_o)\mathbf{c}_o^{o'} - \kappa_r \mathbf{R}(\bar{\theta}_o)\mathbf{c}_o^o, \quad (9b)$$

in which dependencies have been dropped, while (7b) is included and (7a) has to be plugged in.

The dynamic model is derived through the *Euler-Lagrange* formalism. The so-called Lagrange function is given by $\mathcal{L} = \mathcal{T} - \mathcal{U}$, where \mathcal{T} and \mathcal{U} represent the kinetic and potential energies, respectively. The dynamic model equations are then given by $\frac{d}{dt} \frac{\partial \mathcal{L}}{\partial \dot{q}_i} - \frac{\partial \mathcal{L}}{\partial q_i} = \tau_i$, with $i = 1, 2$ and τ_i the associated generalized force acting on the i th generalized coordinate. Given Assumptions 1 and 2, the kinetic and potential energies for a nonprehensile planar rolling manipulation task are $\mathcal{T}(\mathbf{q}, \dot{\mathbf{q}}) = \frac{1}{2} (I_h \dot{\theta}_h^2 + m_o \dot{\mathbf{p}}_o^T(\mathbf{q}, \dot{\mathbf{q}}) \dot{\mathbf{p}}_o(\mathbf{q}, \dot{\mathbf{q}}) + I_o \dot{\theta}_o^2(\mathbf{q})) = \frac{1}{2} \dot{\mathbf{q}}^T \mathbf{B}(\mathbf{q}) \dot{\mathbf{q}}$ and $\mathcal{U}(\mathbf{q}) = m_o g [0 \quad 1] \mathbf{p}_o(\mathbf{q})$, where m_o is the object mass, I_h and I_o are the hand and object inertias, respectively, computed with respect to Σ_h and Σ_o , g is the gravity acceleration (9.81 m/s² is the value employed in Section V), $\mathbf{B}(\mathbf{q}) \in \mathbb{R}^{2 \times 2}$ is the symmetric and positive definite mass matrix whose elements are

$$b_{11}(\mathbf{q}) = I_h + I_o + m_o \boldsymbol{\gamma}^T(\mathbf{q}) \boldsymbol{\gamma}(\mathbf{q}), \quad (10a)$$

$$b_{12}(\mathbf{q}) = b_{21}(\mathbf{q}) = I_o \kappa_r(s_h) + m_o \boldsymbol{\gamma}(\mathbf{q})^T \boldsymbol{\eta}(\mathbf{q}), \quad (10b)$$

$$b_{22}(\mathbf{q}) = I_o \kappa_r^2(s_h) + m_o \boldsymbol{\eta}(\mathbf{q})^T \boldsymbol{\eta}(\mathbf{q}). \quad (10c)$$

By computing the Lagrange equations and considering the Christoffel symbols of the first type [18], the dynamic model can be written as $\mathbf{B}(\mathbf{q})\ddot{\mathbf{q}} + \mathbf{C}(\mathbf{q}, \dot{\mathbf{q}})\dot{\mathbf{q}} + \mathbf{g}(\mathbf{q}) = \boldsymbol{\tau}$, where $\boldsymbol{\tau} = [\tau_h \quad 0]^T$ represents the generalized input force with τ_h the actuating torque around the hand's center of mass; $\mathbf{g}(\mathbf{q}) = [g_1(\mathbf{q}) \quad g_2(\mathbf{q})]^T = \left(\frac{\partial \mathcal{U}(\mathbf{q})}{\partial \mathbf{q}} \right)^T$ and $\mathbf{C}(\mathbf{q}, \dot{\mathbf{q}}) \in \mathbb{R}^{2 \times 2}$ is a suitable matrix whose generic element is given by

$$c_{ij}(\mathbf{q}, \dot{\mathbf{q}}) = \frac{1}{2} \sum_{k=1}^2 \left(\frac{\partial b_{ij}(\mathbf{q})}{\partial q_k} + \frac{\partial b_{ik}(\mathbf{q})}{\partial q_j} + \frac{\partial b_{jk}(\mathbf{q})}{\partial q_i} \right) \dot{q}_k, \quad (11)$$

with $i, j = 1, 2$. By neglecting dependencies, the dynamic model can be written in the following extended form

$$b_{11}\ddot{\theta}_h + b_{12}\ddot{s}_h + c_{11}\dot{\theta}_h + c_{12}\dot{s}_h + g_1 = \tau_h, \quad (12a)$$

$$b_{12}\ddot{\theta}_h + b_{22}\ddot{s}_h + c_{21}\dot{\theta}_h + c_{22}\dot{s}_h + g_2 = 0, \quad (12b)$$

with $g_1 = m_o g \left(-v_h s_{\theta_h} - v_o \frac{\partial c_{\theta_o}}{\partial \theta_h} + u_h c_{\theta_h} - u_o \frac{\partial s_{\theta_o}}{\partial \theta_h} \right)$, and $g_2 = m_o g (v_h' c_{\theta_h} - v_o' c_{\theta_o} - v_o c_{\theta_o}' + u_h' s_{\theta_h} - u_o' s_{\theta_o} - u_o s_{\theta_o}')$, in which (7a) has to be plugged in, the elements of $\mathbf{C}(\mathbf{q}, \dot{\mathbf{q}})$ are omitted for brevity, and c_θ and s_θ are used instead of $\cos \theta$ and $\sin \theta$, respectively.

IV. HYPOTHESES ON THE SHAPES AND INPUT-STATE LINEARIZATION

During experimentation, when highly-g geared harmonic drive plus DC motors are present, the hand's angular acceleration is more convenient than the hand's torque [14]. It is thus suitable to rewrite (12) with $\ddot{\theta}_h = a_h$ as input

$$\ddot{\theta}_h = a_h, \quad (13a)$$

$$\ddot{s}_h = -b_{22}^{-1}(b_{12}a_h + c_{21}\dot{\theta}_h + c_{22}\dot{s}_h + g_2), \quad (13b)$$

where dependencies have been neglected. The equation relating τ_h and a_h is given by

$$\tau_h = \xi(\mathbf{q}, \dot{\mathbf{q}}) + \sigma(\mathbf{q})a_h, \quad (14)$$

with $\xi(\mathbf{q}, \dot{\mathbf{q}}) = g_1 + c_{11}\dot{\theta}_h + c_{12}\dot{s}_h - \frac{b_{12}}{b_{22}}(g_2 + c_{21}\dot{\theta}_h + c_{22}\dot{s}_h)$ and $\sigma(\mathbf{q}) = b_{11} - \frac{b_{12}^2}{b_{22}}$.

Assumption 3: The Coriolis terms $c_{21}(\mathbf{q}, \dot{\mathbf{q}})$ and $c_{22}(\mathbf{q}, \dot{\mathbf{q}})$ are equal to zero.

Remark 1: Looking at (11), Assumption 3 is verified when terms $b_{12} = b_{21}$ and b_{22} in (10b) and (10c), respectively, do not depend on \mathbf{q} , and when b_{11} depends only on θ_h . Looking at the particular expressions of b_{ij} , this means that κ_r has to be constant, i.e. $\kappa_r' = 0$, the combination of the products $\boldsymbol{\gamma}(\mathbf{q})^T \boldsymbol{\eta}(\mathbf{q})$ and $\boldsymbol{\eta}(\mathbf{q})^T \boldsymbol{\eta}(\mathbf{q})$ do not depend on \mathbf{q} , and the product $\boldsymbol{\gamma}(\mathbf{q})^T \boldsymbol{\gamma}(\mathbf{q})$ depends only on θ_h . Considering (6) and (9), the aforementioned properties are thus governed by the shapes of both the hand and the object.

Assumption 3 simplifies (13) as follows

$$\ddot{\theta}_h = a_h, \quad (15a)$$

$$\ddot{s}_h = -\frac{1}{b_{22}}(b_{12}a_h + g_2(\mathbf{q})). \quad (15b)$$

By indicating the state of the system as $\mathbf{x} = [x_1 \quad x_2 \quad x_3 \quad x_4]^T = [\theta_h \quad \dot{\theta}_h \quad s_h \quad \dot{s}_h]^T$, (15) can be written in the affine state-space form (1) with $u = a_h$ and

$$\mathbf{f}(\mathbf{x}) = \begin{bmatrix} x_2 & 0 & x_4 & -\frac{g_2(\mathbf{x})}{b_{22}} \end{bmatrix}^T, \quad (16a)$$

$$\mathbf{b} = \begin{bmatrix} 0 & 1 & 0 & -\frac{b_{12}}{b_{22}} \end{bmatrix}^T. \quad (16b)$$

In order to check whether (15) is input-state linearizable, the controllability matrix $\mathbf{T}(\mathbf{x}) = [\mathbf{b} \quad \text{ad}_{\mathbf{f}} \mathbf{b} \quad \text{ad}_{\mathbf{f}}^2 \mathbf{b} \quad \text{ad}_{\mathbf{f}}^3 \mathbf{b}]$ has to be invertible in a certain region Ω , and the set given by the first three columns of $\mathbf{T}(\mathbf{x})$ has to be involutive (see Theorem 1 in Section II). Taking into account (16), the detailed expression of the controllability matrix is

$$\mathbf{T}(\mathbf{x}) = \begin{bmatrix} 0 & -1 & 0 & 0 \\ 1 & 0 & 0 & 0 \\ 0 & \frac{b_{21}}{b_{22}} & 0 & t_{34} \\ -\frac{b_{21}}{b_{22}} & 0 & t_{43} & t_{44} \end{bmatrix}, \quad (17)$$

with $t_{34} = \frac{1}{b_{22}} \frac{\partial g_2(\mathbf{x})}{\partial x_1} - \frac{b_{12}}{b_{22}^2} \frac{\partial g_2(\mathbf{x})}{\partial x_3}$, $t_{43} = \frac{b_{12}}{b_{22}^2} \frac{\partial g_2(\mathbf{x})}{\partial x_3} - \frac{1}{b_{22}} \frac{\partial g_2(\mathbf{x})}{\partial x_1}$, and $t_{44} = x_4 \frac{b_{12}}{b_{22}} \frac{\partial^2 g_2(\mathbf{x})}{\partial x_3^2} - \frac{x_2}{b_{22}} \frac{\partial^2 g_2(\mathbf{x})}{\partial x_1^2}$.

Defining the region $\Omega = \left\{ \mathbf{x} \in \mathbb{R}^4 : \frac{\partial g_2(\mathbf{x})}{\partial x_1} \neq \frac{b_{12}}{b_{22}} \frac{\partial g_2(\mathbf{x})}{\partial x_3} \right\}$, it is possible to prove that $\mathbf{T}(\mathbf{x})$ in (17) is made by linearly independent columns: the first three of them build an involutive set (proofs are omitted for brevity). The system (15) is then input-state linearizable in Ω .

To render (15) in the normal form (2), a diffeomorphism $\phi(\mathbf{x})$ (4) has to be found. Hence, in order to compute the first component z_1 , equations (3) have to hold for the vector fields (16). In particular, looking at the expression of the first three columns of $\mathbf{T}(\mathbf{x})$, condition (3a) yields $\frac{\partial z_1}{\partial x_2} - \frac{b_{12}}{b_{22}} \frac{\partial z_1}{\partial x_4} = 0$, $\frac{b_{12}}{b_{22}} \frac{\partial z_1}{\partial x_3} - \frac{\partial z_1}{\partial x_1} = 0$, and $\frac{\partial z_1}{\partial x_4} t_{43} = 0$. The solution to this system is then given by $z_1 = \frac{b_{12}}{b_{22}} x_1 + x_3$. It is easy to verify that such a choice for z_1 also satisfies (3b). Therefore, the complete diffeomorphism is given by

$$\phi(\mathbf{x}) = \begin{bmatrix} z_1 \\ z_2 \\ z_3 \\ z_4 \end{bmatrix} = \begin{bmatrix} y \\ \dot{y} \\ \ddot{y} \\ y^{(3)} \end{bmatrix} = \begin{bmatrix} \frac{b_{12}}{b_{22}} x_1 + x_3 \\ \frac{b_{12}}{b_{22}} x_2 + x_4 \\ -\frac{g_2(\mathbf{x})}{b_{22}} \\ -\frac{1}{b_{22}} \left(\frac{\partial g_2(\mathbf{x})}{\partial x_1} x_2 + \frac{\partial g_2(\mathbf{x})}{\partial x_3} x_4 \right) \end{bmatrix}, \quad (18)$$

where $y^{(j)}$ is the j th-order derivative, with $j \geq 3$. Considering (5), the input transformation $a_h = \alpha(\mathbf{x}) + \beta(\mathbf{x})v$ finally renders (15) in the normal form (2), with

$$\alpha(\mathbf{x}) = -\frac{\left(\frac{\partial^2 g_2(\mathbf{x})}{\partial x_1^2} x_2 - \frac{g_2(\mathbf{x})}{b_{22}} \frac{\partial g_2(\mathbf{x})}{\partial x_3} + \frac{\partial^2 g_2(\mathbf{x})}{\partial x_3^2} x_4 \right)}{\left(\frac{\partial g_2(\mathbf{x})}{\partial x_1} - \frac{b_{12}}{b_{22}} \frac{\partial g_2(\mathbf{x})}{\partial x_3} \right)}, \quad (19a)$$

$$\beta(\mathbf{x}) = -b_{22} \left(\frac{\partial g_2(\mathbf{x})}{\partial x_1} - \frac{b_{12}}{b_{22}} \frac{\partial g_2(\mathbf{x})}{\partial x_3} \right)^{-1}. \quad (19b)$$

This is the core result since, under Assumptions 1, 2 and 3, a general diffeomorphism is found to change a nonprehensile 2D rolling manipulation system into a normal form where simple linear controllers can be applied.

Therefore, in general, any suitable approach can be employed to control the normal form (2). The exact feedforward linearization (EFL) technique [9] is here considered. In detail, a change of coordinates is applied to (15) through (18). To get the normal form, the EFL technique does not use the feedback transformation $a_h = \alpha(\mathbf{x}) + \beta(\mathbf{x})v$, but $a_h = \alpha(\mathbf{x}^*) + \beta(\mathbf{x}^*)v$, where \mathbf{x}^* is the desired state¹ (in feedforward). The new virtual input v is instead designed as an extended PID ^{$n-1$} plus a feedforward action

$$v = z_4^* + \sum_{i=0}^4 k_i e_i, \quad (20a)$$

$$e_0 = \int_0^t e_1(\tau) d\tau, \quad (20b)$$

$$e_i = z_i^* - z_i, \quad (20c)$$

¹Eventually retrieved from \mathbf{z}^* through ϕ^{-1} .

with k_i positive gains such that the resulting characteristic polynomial is Hurwitz.

Remark 2: A SISO input-state linearizable system is also differentially flat with output $y = h(\mathbf{x}) = z_1$ (see Appendix). Therefore, given Assumptions 1, 2 and 3, a nonprehensile planar rolling manipulation system is differentially flat with flat output $y = \frac{b_{12}}{b_{22}} x_1 + x_3$. For both motion planning and controlling purposes under differential flatness theory, it is essential to express the state \mathbf{x} and input a_h as function of y and its derivatives (see (22) in Appendix). In many cases this might be cumbersome. Even if it is possible to use some symbolic mathematical computation software, some guidelines are provided in the following. The first step is to write $x_3 = y - \frac{b_{12}}{b_{22}} x_1$ and $x_4 = \dot{y} - \frac{b_{12}}{b_{22}} x_2$ from (18). Later, substitute x_3 and x_4 from the previous step in the last row of (18) and solve for x_2 . Plug x_3 from the first step in $\ddot{y} = -\frac{g_2(\mathbf{x})}{b_{22}}$ and solve for x_1 (this will be function of only y and \dot{y}). Substitute back x_1 in x_2 and, in turn, in x_3 and x_4 from previous steps (it comes out that x_3 depends only on y and \dot{y} , while x_2 and x_4 are generally function of y , \dot{y} , \ddot{y} and $y^{(3)}$). Finally, it is possible to express a_h as function of y and its derivatives by considering $a_h = \alpha(\mathbf{x}) + \beta(\mathbf{x})y^{(4)}$ from (2b), and substituting x_i , with $i = 1, \dots, 4$, from the previous steps. Notice that not every desired trajectory can be imposed to y . As it will be highlighted in the case studies, some desired behaviours could make unbounded the state of a nonprehensile planar rolling manipulation system.

V. CASE STUDIES

A. Ball and beam

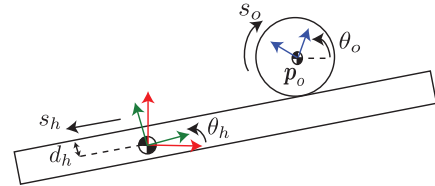


Fig. 2. A representation of the ball and beam system. In red the world fixed frame Σ_w . In green the hand frame Σ_h , while in blue the object frame Σ_o , placed at the respective centres of mass.

1) *Formulation:* Referring to Fig. 2, the beam can rotate around its center of mass while the ball can only roll along the beam. The shape of the hand, *i.e.* the beam, is parametrized through $c_h^h(s_h) = [-s_h \quad d_h]^T$, with $d_h \in \mathbb{R}^+$ a fixed distance between the beam's center of mass and its surface where the ball rolls. The ball's shape is parametrized by $c_o^o(s_h) = -\rho_o \left[\sin \frac{s_h}{\rho_o} \quad \cos \frac{s_h}{\rho_o} \right]^T$, with $\rho_o \in \mathbb{R}^+$ the radius of the ball. Considering (6), the signed curvatures of the beam and the ball are $\kappa_h = 0$ and $\kappa_o = -1/\rho_o$, respectively. The relative curvature is thus given by $\kappa_r = 1/\rho_o$. The ball's angular velocity is instead given by (7b) $\dot{\theta}_o = \dot{\theta}_h + \frac{\dot{s}_h}{\rho_o}$. In order to compute the mass matrix of the system, the vectors $\gamma(\mathbf{q})$ and $\eta(\mathbf{q})$ in (9) are $\gamma(\mathbf{q}) = [-(\rho_o + d_h)c_{\theta_h} + s_h s_{\theta_h} \quad -(\rho_o + d_h)s_{\theta_h} - s_h c_{\theta_h}]^T$, and $\eta(\mathbf{q}) = -[c_{\theta_h} \quad s_{\theta_h}]^T$. Therefore, the parameters in (12)

are $b_{11} = I_h + I_o + m_o d_h^2 + 2m_o d_h \rho_o + m_o \rho_o^2 + m_o s_h^2$, $b_{12} = b_{21} = \frac{I_o}{\rho_o} + m_o d_h + m_o \rho_o$, $b_{22} = \frac{I_o}{\rho_o^2} + m_o$, $c_{11} = m_o s_h \dot{s}_h$, $c_{12} = m_o s_h \dot{\theta}_h$, $c_{21} = m_o s_h \dot{\theta}_h$, $c_{22} = 0$, $g_1 = -m_o g ((d_h + \rho_o) \sin \theta_h + s_h \cos \theta_h)$ and $g_2 = -m_o g \sin \theta_h$. Considering the acceleration a_h of the beam as input, the system can be written as in (13), with τ_h as in (14). However, it is possible to verify that Assumption 3 is not verified for the ball and beam case since $c_{21} \neq 0$. Even if κ_r is constant and the products $\gamma(\mathbf{q})^T \eta(\mathbf{q})$ and $\eta(\mathbf{q})^T \eta(\mathbf{q})$ do not depend on \mathbf{q} , the product $\gamma(\mathbf{q})^T \eta(\mathbf{q})$ does not depend only on θ_h , but it depends on the arclength parameter. Therefore, the ball and beam system is not input-state linearizable. This result is well known in the literature, nevertheless, in many cases it is possible to approximate c_{21} to zero [7]. This is true for small velocities of the beam, small masses of the ball and not so long beam. Hence, by putting $c_{21} = 0$, only for control design purposes, it is possible to write the approximated ball and beam system like in (15). The affine state space form of the approximated ball and beam system has the following

vector fields (16) $\mathbf{f}(\mathbf{x}) = \begin{bmatrix} x_2 & 0 & x_4 & \frac{m_o \rho_o^2 g \sin x_1}{I_o + m_o \rho_o^2} \end{bmatrix}^T$ and $\mathbf{b} = \begin{bmatrix} 0 & 1 & 0 & -\rho_o \frac{m_o \rho_o^2 + d_h m_o \rho_o + I_o}{I_o + m_o \rho_o^2} \end{bmatrix}^T$. Computing the matrix $\mathbf{T}(\mathbf{x})$ as in (17), it is possible to verify that the approximate dynamic model is input-state linearizable in the region $\Omega = \{\mathbf{x} \in \mathbb{R}^4 : \cos \theta_h \neq 0 \Rightarrow |\theta_h| < \frac{\pi}{2}\}$. Notice that such a region is not restrictive because, with no bound on other states, Ω covers all practical situations since outside it the ball falls down from the hand. Finally, it is possible to compute the diffeomorphism (18) $\phi(\mathbf{x}) = \begin{bmatrix} \frac{b_{12}}{b_{22}} x_1 + x_3 & \frac{b_{12}}{b_{22}} x_2 + x_4 & \frac{m_o g}{b_{22}} \sin x_1 & \frac{m_o g x_2}{b_{22}} \cos x_1 \end{bmatrix}^T$, yielding the normal form

$$\dot{z}_1 = z_2, \quad (21a)$$

$$\dot{z}_2 = z_3, \quad (21b)$$

$$\dot{z}_3 = z_4, \quad (21c)$$

$$\dot{z}_4 = \beta(\mathbf{x})|_{\mathbf{x}=\phi^{-1}(\mathbf{z})}^{-1} (a_h - \alpha(\mathbf{x})|_{\mathbf{x}=\phi^{-1}(\mathbf{z})}), \quad (21d)$$

with $\alpha(\mathbf{x}) = m_o g x_2 \tan x_1$ and $\beta(\mathbf{x}) = \frac{b_{22}}{m_o g \cos x_1}$ from (19). The control is then performed with the EFL technique described in Section IV.

For the differential flatness, the flat output is $y = h(\mathbf{x}) = \frac{b_{12}}{b_{22}} x_1 + x_3$. Following the steps in Remark 2, the state variables can be then expressed as function of y and its derivatives $x_1 = \text{asin}\left(\frac{b_{22} \ddot{y}}{m_o g}\right)$, $x_2 = \frac{b_{22} \dot{y}^{(3)}}{m_o g \cos\left(\text{asin}\left(\frac{b_{22} \ddot{y}}{m_o g}\right)\right)}$, $x_3 = y - \frac{b_{12}}{b_{22}} \text{asin}\left(\frac{b_{22} \ddot{y}}{m_o g}\right)$ and $x_4 = \dot{y} - \frac{b_{12} \dot{y}^{(3)}}{m_o g \cos\left(\text{asin}\left(\frac{b_{22} \ddot{y}}{m_o g}\right)\right)}$.

Remark 3: Notice that within this framework it is not possible to choose as flat output only the arclength parameter as usually done in the literature [7], [9]. This is because the dynamic model of the ball and beam system here derived is slightly different from [7] since it takes into account the distance d_h between the hand's center of mass and the rolling surface. An approximation to neglect the hand and put Σ_w aligned with the ball's center of mass is instead usually considered: this yields $b_{12} = 0$, meaning that

$m_o \gamma(\mathbf{q})^T \eta(\mathbf{q}) = -I_o \kappa_r (s_h)$. Such approximation, verified to be effective in the practice in the above cited papers, is not considered here since the scope of such a work is to consider a general framework for nonprehensile planar rolling manipulation in which the assumption of $b_{12} = 0$ would be too much restrictive and valid only for the ball and beam case. The price to pay is the impossibility to have as flat output $y = s_h = x_3$. However, since $x_3 = y - \frac{b_{12}}{b_{22}} \text{asin}\left(\frac{b_{22} \ddot{y}}{m_o g}\right)$, with $y = \frac{b_{12}}{b_{22}} x_1 + x_3$, it is possible to approximate $y \simeq x_3$ when $b_{22} \gg b_{12}$.

2) *Simulations:* Simulations are performed for the ball and beam system. The control law has been designed with reference to the approximated model with $c_{21} = 0$. The ball and beam dynamic system, instead, has been simulated without such approximation. The value employed to simulate the effective ball and beam system are: $m_o = 0.5$ kg, $\rho_o = 10$ cm, $I_h = 0.2$ kg m², $d_h = 1$ cm and $I_o = m_o \rho_o^2$. To emulate parameter uncertainties, such values have been augmented of the 5% in the control law. A time delay of about 0.01 s is considered for the measurements.

As a first task, the hand starts at the desired condition $\theta_h^* = 0$, but the ball is placed at $s_h = -1$ m while its desired configuration is at $s_h^* = 0$. The initial and desired velocities for both the hand and the arclength parameter are 0. Looking at the diffeomorphism $\phi(\mathbf{x})$, the goal can be achieved through $\mathbf{z}^* = \mathbf{0}$. The control gains k_i with $i = 0, \dots, 4$ in (20a) have been chosen as (0.01, 81, 108, 54, 12), respectively. The errors e_i in (20c) asymptotically go to zero as shown in Fig. 3(a), meaning that the state \mathbf{z} tends to zero. As previously highlighted, this means also that the state $\mathbf{x} = [\theta_h \ \dot{\theta}_h \ s_h \ \dot{s}_h]^T$ goes to zero as desired: this is depicted in Fig. 3(b). The behaviour of the torque τ_h in (14) is represented in Fig. 3(c). The time history does not start from zero since at the beginning the ball is not aligned with the hand's center of mass causing a torque around this last. The balancing task is then satisfied despite the control law has been designed on an approximate system with parameters uncertainty.

As noticed in Remark 3, it is not possible to impose a desired behaviour directly to $s_h = x_3$, but to $y = \frac{b_{12}}{b_{22}} x_1 + x_3$. However, since the chosen parameters (not so far from a real system) are such that $b_{22} \gg b_{12}$, it is a good approximation to impose the reference behaviour for s_h to y . As a second test, it is then desired that $z_1^* = y^* = 0.05 \cos t$, with t the time. The desired values for z_i^* , with $i = 2, \dots, 4$, are the time time derivatives of y^* . The control gains are chosen like the previous test, while initially the ball is placed at $s_h = -10$ cm. Again, the errors e_i in (20c) go asymptotically to zero as shown in Fig. 4(a). Fig. 4(b) shows that the time history of s_h follows the desired trajectory given to y^* , validating the considered approximation. Therefore, under the conditions given in Remark 3, differential flatness can be employed also under this framework as in literature [7], [9]. The behaviour of τ_h in (14) is represented in Fig. 4(c). Again, the related plot does not start from zero because of the misalignment of the ball with respect to the hand's center

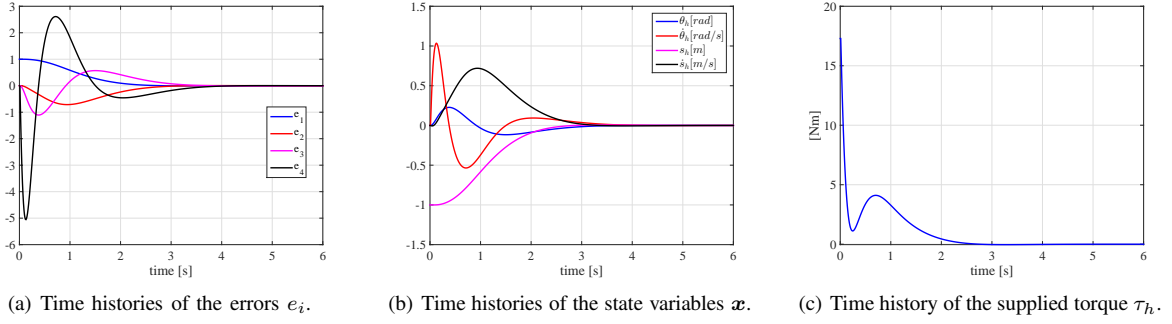


Fig. 3. Time histories related to the first simulation test about the ball and beam system.

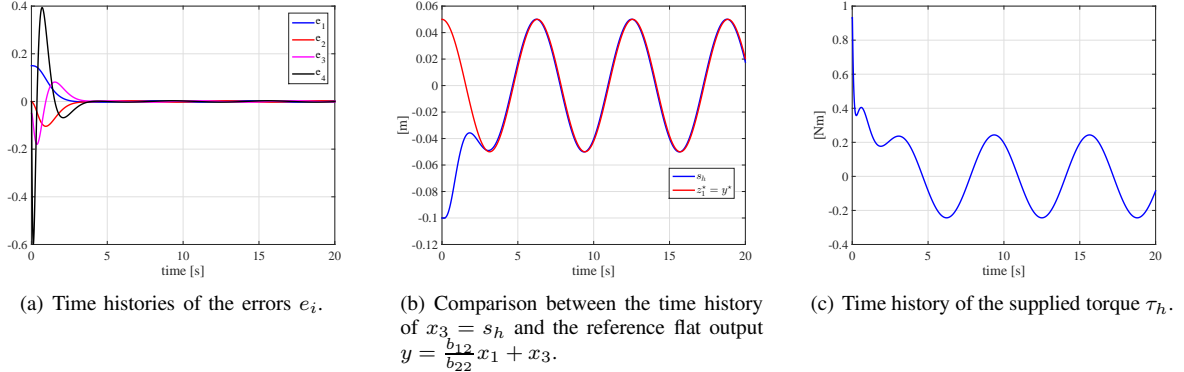


Fig. 4. Time histories related to the second simulation test about the ball and beam system.

of mass.

Finally, notice that it is not possible to stabilize the ball with a non-zero beam's angle. Looking at the dynamic model, this requires a constant torque resulting in unbounded velocities.

B. Disk on disk (DoD)

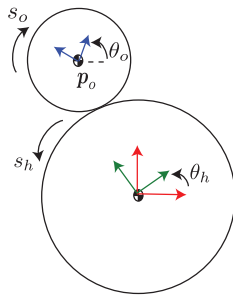


Fig. 5. A representation of the disk on disk system. In red the world fixed frame Σ_w . In green the hand frame Σ_h , while in blue the object frame Σ_o , placed at the respective centres of mass.

1) *Formulation*: This case study considers the balancing of a disk free to roll on an actuated disk. Referring to Fig. 5, the shape of the hand, *i.e.* the actuated disk, is parametrized by $c_h^h(s_h) = \rho_h \left[-\sin \frac{s_h}{\rho_h} \cos \frac{s_h}{\rho_h} \right]^T$, with $\rho_h \in \mathbb{R}^+$ the radius of the hand. The upper disk's shape is parametrized as in the previous case study. Considering (6), the relative curvature is given by $\kappa_r = \frac{\rho_h + \rho_o}{\rho_h \rho_o}$. The

upper disk angular velocity is given by $\dot{\theta}_o = \dot{\theta}_h + \kappa_r \dot{s}_h$. The vectors $\gamma(q)$ and $\eta(q)$ are computed like in (9): $\gamma(q) = -(\rho_h + \rho_o) \left[\cos \left(\theta_h + \frac{s_h}{\rho_h} \right) \sin \left(\theta_h + \frac{s_h}{\rho_h} \right) \right]^T$, and $\eta(q) = -\rho_o \kappa_r \left[\cos \left(\theta_h + \frac{s_h}{\rho_h} \right) \sin \left(\theta_h + \frac{s_h}{\rho_h} \right) \right]^T$. Therefore, the parameters in (12) are $b_{11} = I_h + I_o + m_o(\rho_h + \rho_o)^2$, $b_{12} = b_{21} = I_o \kappa_r + m_o \frac{(\rho_h + \rho_o)^2}{\rho_h}$, $b_{22} = I_o \kappa_r^2 + m_o \rho_o^2 \kappa_r^2$, $c_{11} = c_{12} = c_{21} = c_{22} = 0$, $g_1 = -m_o g (\rho_h + \rho_o) \sin \left(\theta_h + \frac{s_h}{\rho_h} \right)$ and $g_2 = -m_o g \rho_o \kappa_r \sin \left(\theta_h + \frac{s_h}{\rho_h} \right)$. Notice that the quantity $\theta_h + \frac{s_h}{\rho_h}$ is the angle of the object's center of mass with respect to the vertical axis of Σ_w . It is possible to verify that the DoD dynamic model fully verifies Assumption 3. Hence, considering the acceleration a_h of the actuated disk as input, the DoD dynamics can be written as in (15) with τ_h as in (14). The affine state space form assumes the following vector fields (16) $f(x) = \begin{bmatrix} x_2 & 0 & x_4 & \frac{m_o g \rho_o \sin \left(x_1 + \frac{x_3}{\rho_h} \right)}{I_o \kappa_r + m_o \rho_o^2 \kappa_r} \end{bmatrix}^T$ and $b = \begin{bmatrix} 0 & 1 & 0 & -\frac{m_o \rho_o^2 + m_o \rho_h \rho_o + I_o}{\kappa_r (m_o \rho_o^2 + I_o)} \end{bmatrix}^T$. Computing the matrix $T(x)$ as in (17), it is possible to verify that the approximate dynamic model is input-state linearizable in the region $\Omega = \{x \in \mathbb{R}^4 : \cos \left(x_1 + \frac{x_3}{\rho_h} \right) \neq 0 \Rightarrow |x_1 + \frac{x_3}{\rho_h}| < \frac{\pi}{2}\}$. Notice that such a region is not restrictive because, with no bound on other states, Ω covers all practical situations since outside it the disk falls down from the hand. Finally, diffeomorphism (18) is

$$\phi(\mathbf{x}) = \begin{bmatrix} \frac{b_{12}}{b_{22}}x_1 + x_3 & \frac{b_{12}}{b_{22}}x_2 + x_4 & \frac{m_o g \rho_o \sin\left(x_1 + \frac{x_3}{\rho_h}\right)}{I_o \kappa_r + m_o \rho_o^2 \kappa_r} \\ m_o g \rho_o \kappa_r \left(x_2 + \frac{x_4}{\rho_h}\right) \cos\left(x_1 + \frac{x_3}{\rho_h}\right) \end{bmatrix}^T, \quad \text{with} \quad \alpha(\mathbf{x}) = \frac{\sin\left(x_1 + \frac{x_3}{\rho_h}\right) x_2 - \left(\frac{m_o g \rho_o \kappa_r}{b_{22} \rho_h} \sin\left(x_1 + \frac{x_3}{\rho_h}\right) + \frac{x_4}{\rho_h^2}\right) \cos\left(x_1 + \frac{x_3}{\rho_h}\right)}{\left(1 - \frac{b_{12}}{b_{22} \rho_h}\right) \cos\left(x_1 + \frac{x_3}{\rho_h}\right)} \quad \text{and}$$

$\beta(\mathbf{x}) = b_{22} \left(m_o g \rho_o \kappa_r \left(1 - \frac{b_{12}}{b_{22} \rho_h}\right) \cos\left(x_1 + \frac{x_3}{\rho_h}\right)\right)^{-1}$. The control is again performed with the EFL technique described in Section IV.

Within differential flatness, the flat output is $y = h(\mathbf{x}) = \frac{b_{12}}{b_{22}}x_1 + x_3$. Following Remark 2, the state variables can be expressed as function of y and its derivatives. Only $x_1 = \left(1 - \frac{b_{12}}{b_{22} \rho_h}\right)^{-1} \left(\text{asin}\left(\frac{I_o \kappa_r + m_o \rho_o^2 \kappa_r}{m_o g \rho_o} \ddot{y}\right) - \frac{y}{\rho_h}\right)$ and $x_3 = y - \frac{b_{12} \rho_h}{b_{22} \rho_h - b_{12}} \left(\text{asin}\left(\frac{I_o \kappa_r + m_o \rho_o^2 \kappa_r}{m_o g \rho_o} \ddot{y}\right) - \frac{y}{\rho_h}\right)$ are here expressed for brevity.

Remark 4: Notice that in this case study the only possibility of balancing is with the object directly above the hand's center of mass, *i.e.* $\theta_h + \frac{s_h}{\rho_h} = 0$. As noticed in [14], any other balancing position leads to constant angular acceleration resulting in unbounded velocities. The differential flatness loses thus some sense for the disk on disk.

Looking at $\phi(\mathbf{x})$, stabilizing the origin $\mathbf{z} = \mathbf{0}$ is equivalent to stabilizing $\mathbf{x} = \mathbf{0}$ and then $x_1 + \frac{x_3}{\rho_h} = 0$. However, notice that through the following further change of coordinates $\bar{\mathbf{z}} = \begin{bmatrix} z_1 - \left(\frac{b_{12} - b_{22} \rho_h}{b_{22}} \theta_h^*\right) & z_2 & z_3 & z_4 \end{bmatrix}^T$ it is possible to balance the object with θ_h at a desired constant angle $\theta_h^* = x_1^*$. It is easy to verify that such additional diffeomorphism does not change the normal form (2) expressed now in terms of $\bar{\mathbf{z}}$. With some algebra, it is possible to show that stabilizing the origin $\bar{\mathbf{z}} = \mathbf{0}$ yields $x_1 = x_1^*$, $x_1 + \frac{x_3}{\rho_h} = 0$ and $x_2 = x_4 = 0$.

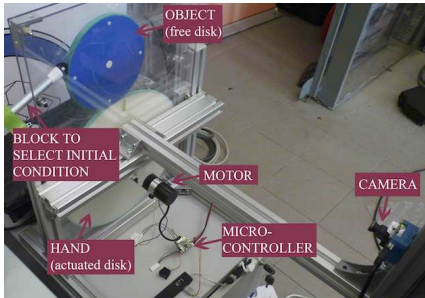


Fig. 6. Experimental prototype of the disk-on-disk system available at PRISMA Lab.

2) *Experiments:* Performance are evaluated through some experiments by using the experimental disk on disk prototype shown in Fig 6. The hand is actuated by a DC motor (Harmonic Drive RH-8D 3006) equipped with a harmonic drive whose gearhead ratio is 100 : 1. Rubber bands of small thickness encircle both the object and the hand. The commands to the motor are provided by an ARM CORTEX M3 microcontroller (32 bit, 75 MHz). The microcontroller receives current references from an external PC through a USB cable. The output of the microcontroller is the current

reference for the motor servo, which is transformed in torque for the hand disk. Therefore, the control v in (20a) is first transformed in $a_h = \alpha(\mathbf{x}^*) + \beta(\mathbf{x}^*)v$ and then in τ_h as in (14). Finally τ_h has to be transformed through a current control law as $i_{com} = (1/\varsigma_m)(\tau_h + \mu_d \dot{\theta}_h + f_s \text{sgn}(\dot{\theta}_h)) + k_p(\theta_h^d - \theta_h) + k_d(\dot{\theta}_h^d - \dot{\theta}_h)$, where θ_h^d and $\dot{\theta}_h^d$ are the desired hand position and velocity, respectively, obtained by integrating a_h ; k_p and k_d are two gains, set to 10 and 1, respectively, during the experiments; $\varsigma_m = 4.2$ is the motor constant available from the motor data-sheet; $\mu_d = 0.29$ is a viscous coefficient and $f_s = 0.3$ is the torque required to overcome friction at rest. These two last parameters have been experimentally identified. In addition, the microcontroller also provides the measured position of the hand to the external PC. The position of the upper disk, instead, is given by an external visual system. This consists of a uEye UI-122-xLE camera providing (376×240) pixel images to the PC at 75 Hz, that is also the controller sample rate. With respect to [13], [14] this is a slower sample time. Moreover, with respect again to the two above cited works, the employed set-up is mounted in full gravity between two plexiglass plates. Finally, the other parameters are $\rho_h = 15$ cm, $\rho_o = 7.5$ cm, $m_o = 16$ g, $I_h = 5.3 \cdot 10^{-3}$ kg m² and $I_o = 12.15 \cdot 10^{-5}$ kg m², while the control gains k_i , with $i = 0, \dots, 4$, in (20a) are (0.7, 180, 70, 110, 10).

Experiments are focused on the balancing of the object on the upright unstable position. A video of the performed experiments is present in the multimedia attachment, along with the case of stabilizing the angle of the hand at a desired θ_h^* . Since θ_h starts from 0 and the upper disk starts at about $\theta_h + \frac{s_h}{\rho_h} = 5$ degrees with respect to the vertical axis of Σ_w , then s_h has an initial value of 1.57 cm. Therefore, to stabilize the upright unstable position, the desired values for the normal form state system is $\mathbf{z}^* = \mathbf{0}$: this yields $\mathbf{x}^* = \mathbf{0}$ and then $\theta_h + \frac{s_h}{\rho_h} = 0$. After the stabilization, the object has been voluntarily perturbed by pushing it away from the balancing position: the control law is able to recover such perturbation as shown in the time histories of Fig. 7. The time histories of e_i in (20c) go to zero as in Fig. 7(a). The oscillations are because of the noisy visual measurements and the numerical derivation, without filtering, performed to obtain the velocity measurements of $\dot{\theta}_h$, from the encoder, and \dot{s}_h , from the visual system. As mentioned above, since \mathbf{z} goes to zero, also \mathbf{x} goes to zero as represented in Fig. 7(b). The time history of the angle $\theta_h + \frac{s_h}{\rho_h}$ of the object's center of mass with respect to the vertical axis of Σ_w is depicted in Fig. 7(c): the balancing task is then successfully achieved.

It is worth highlighting that an input-state linearization technique for the sole DoD system is presented in [14]. Nevertheless, another change of coordinate is performed in that paper before applying the final diffeomorphism, while an exact feedback linearization control is used instead of the EFL approach here employed.

VI. CONCLUSION AND FUTURE WORK

A general framework to control nonprehensile planar rolling dynamic manipulation systems has been derived in

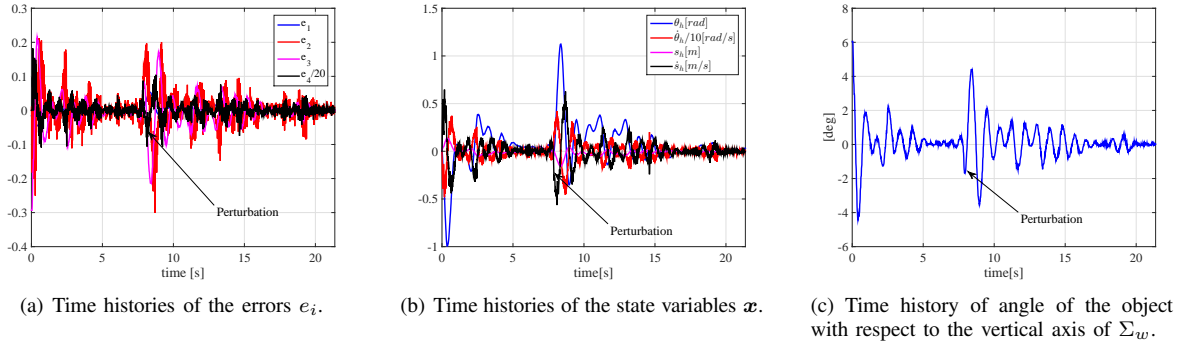


Fig. 7. Time histories related to the first simulation test about the disk on disk system.

this paper. In particular, a dynamic model for these tasks has been introduced. Under certain assumptions on both the hand and the object shapes, these systems are input-state linearizable with output $y = \frac{b_{12}}{b_{22}}\theta_h + s_h$. A connection with the differential flatness theory has been also highlighted. Simulation and experiments for two case studies have been presented. The proposed method works also in cases where the considered assumptions are not fully verified. Future work is devoted to removing Assumptions 2 and 3.

APPENDIX

The single-input system (1) is *differentially flat* [19], [20] if, and only if, there exists a *flat output* $y = h(x) \in \mathcal{C}^n$ such that it is possible to express the state and the input as function of the flat output and its derivatives

$$x = \delta(y, \dot{y}, \dots, y^{(n-1)}), \quad (22a)$$

$$u = \psi(y, \dot{y}, \dots, y^{(n)}), \quad (22b)$$

where $\delta : \mathbb{R} \times \dots \times \mathbb{R} \rightarrow \mathbb{R}^n$ and $\psi : \mathbb{R} \times \dots \times \mathbb{R} \rightarrow \mathbb{R}$ are smooth functions at least in an open set of \mathbb{R}^n and \mathbb{R}^{n+1} , respectively. Differentially flat systems are useful when explicit trajectory generation is required since it is possible to determine the full behaviour of the system from the flat output and its derivatives. It is then possible to map them in the proper input by considering the nominal control $u^* = \psi(y^*, \dot{y}^*, \dots, y^{*(n)})$ in feedforward, where y^* is the desired behaviour of the flat output. The exact feedback linearizability (*i.e.*, conditions of Theorem 1 are verified and it is possible to find the diffeomorphism $\phi(x)$ as in (4)) is a necessary and sufficient condition for flatness of a system [19]. Therefore, each system (1) that is input-state linearizable and that can be transformed in the normal form (2) through the diffeomorphism (4) is also a differentially flat system with flat output $y = h(x) = z_1$, and in which relations (22) hold.

REFERENCES

- [1] K. M. Lynch and M. T. Mason, "Dynamic nonprehensile manipulation: Controllability, planning, and experiments," *International Journal of Robotics Research*, vol. 18, no. 1, pp. 64–92, 1999.
- [2] M. T. Mason, "Progress in nonprehensile manipulation," *International Journal of Robotics Research*, vol. 18, no. 11, pp. 1129–1141, 1999.
- [3] M. Lynch, K. and T. D. Murphey, "Control of nonprehensile manipulation," in *Control Problems in Robotics*, ser. Springer Tracts in Advanced Robotics, A. Bicchi, D. Prattichizzo, and H. Christensen, Eds. Springer Berlin Heidelberg, 2003, vol. 4, pp. 39–57.
- [4] Z. Li and J. Canny, "Motion of two rigid bodies with rolling constraint," *IEEE Transactions on Robotics and Automation*, vol. 6, no. 1, pp. 62–72, 1990.
- [5] S. Awatar, C. Bernard, N. Boklund, A. Master, D. Ueda, and K. Craig, "Mechatronic design of a ball-on-plate balancing system," *Mechatronics*, vol. 12, no. 2, pp. 217–228, 2002.
- [6] J. H. Park and Y. J. Lee, "Robust visual servoing for motion control of the ball on a plate," *Mechatronics*, vol. 13, no. 7, pp. 723–738, 2003.
- [7] J. Hauser, S. Sastry, and P. Kokotovic, "Nonlinear control via approximate input-output linearization: The ball and beam example," *IEEE Transactions on Automatic Control*, vol. 37, no. 3, pp. 392–398, 1992.
- [8] A. Teel and L. Praly, "Tools for semiglobal stabilization by partial state and output feedback," *SIAM Journal on Control and Optimization*, vol. 33, no. 5, pp. 1443–1488, 1995.
- [9] V. Hagenmeyer, S. Streif, and M. Zeitz, "Flatness-based feedforward and feedback linearisation of the ball & plate lab experiment," in *Proceedings of the 6th IFAC-Symposium on Nonlinear Control Systems*, 2004.
- [10] K. M. Lynch, N. Shiroma, H. Arai, and K. Tanie, "The roles of shape and motion in dynamic manipulation: The butterfly example," in *1998 IEEE International Conference on Robotics and Automation*, Leuven, B, 1998, pp. 1958–1963.
- [11] M. Cefalo, L. Lanari, and G. Oriolo, "Energy-based control of the butterfly robot," in *8th International IFAC Symposium on Robot Control*, Bologna, I, 2006, pp. 1–6.
- [12] M. Surov, A. Shiriaev, L. Freidovich, S. Gusev, and L. Paramonov, "Case study in non-prehensile manipulation: Planning perpetual rotations for "Butterfly" robot," in *2015 IEEE International Conference on Robotics and Automation*, Seattle, WA, USA, 2015, pp. 1484–1489.
- [13] J.-C. Ryu, F. Ruggiero, and K. M. Lynch, "Control of nonprehensile rolling manipulation: Balancing a disk on a disk," in *2012 IEEE International Conference on Robotics and Automation*, St. Paul, MN, USA, 2012, pp. 3232–3237.
- [14] J.-C. Ryu, F. Ruggiero, and K. M. Lynch, "Control of nonprehensile rolling manipulation: Balancing a disk on a disk," *IEEE Transactions on Robotics*, vol. 29, no. 5, pp. 1152–1161, 2013.
- [15] B. Kiss, J. Lévine, and B. Lantos, "On motion planning for robotic manipulation with permanent rolling contacts," *International Journal of Robotics Research*, vol. 21, no. 5–6, pp. 443–461, 2002.
- [16] D. Hristu-Varsakelis, "The dynamics of a forced sphere plate mechanical system," *IEEE Transactions on Automatic Control*, vol. 46, no. 5, pp. 678–686, 2001.
- [17] J.-J. E. Slotine and W. Li, *Applied Nonlinear Control*. Prentice-Hall Englewood Cliffs, NJ, 1991.
- [18] B. Siciliano, L. Sciacivco, L. Villani, and G. Oriolo, *Robotics: Modelling, Planning and Control*. London, UK: Springer, 2009.
- [19] M. Fliess, P. Levine, and P. Rouchon, "Flatness and defect of nonlinear systems: Introductory theory and examples," *International Journal of Control*, vol. 61, pp. 1327–1361, 1995.
- [20] M. Fliess, P. Levine, and P. Rouchon, "A Lie-Backlund approach to equivalence and flatness of nonlinear systems," *IEEE Transactions on Automatic Control*, vol. 44, pp. 922–937, 1999.